Fusion Engineering and Design 220 (2025) 115357

Contents lists available at ScienceDirect

Fusion Engineering and Design

journal homepage: www.elsevier.com/locate/fusengdes

# Optimisation of STEP poloidal field coils with superconducting coil constraints in STEP-Bluemira power plant design framework

Athoy Nilima [a,*], Matthew Bluteau [a], James Cook [a], Oliver Funk [a], Georgina Graham [a], Jonathan Matthews [a], Stuart I. Muldrew [b], Alexander J. Pearce [b], Dario Vaccaro [a]

[a] UK Atomic Energy Authority, Culham Campus, Abingdon, Oxfordshire, OX14 3DB, UK
[b] UK Industrial Fusion Solutions Ltd, Culham Campus, Abingdon, Oxfordshire, OX14 3DB, UK

ARTICLE INFO

*Keywords:*
Spherical tokamak
STEP
Bluemira
Fusion powerplant
System codes
Design framework

ABSTRACT

The Spherical Tokamak for Energy Production (STEP) programme aims to deliver a UK prototype fusion energy plant, targeting 2040, and a path to commercial viability of fusion. The conceptual design of such a prototype, meeting engineering and physics constraints, is complex due to the compact nature of spherical tokamaks. The STEP-Bluemira design framework addresses these challenges by providing optimisation tools that simplify the design process, enabling a rapid, integrated workflow for quick evaluation and improvement of design concepts. This work reports recent progress in the STEP-Bluemira power plant design framework, focusing on newly added capabilities for nested optimisation of poloidal field (PF) coil positions and currents with critical current constraints. A keep-in-zone module is introduced, that defines regions for PF coils based on spatial compatibility with the central solenoid, toroidal field coils, and other components. New methods for calculating critical current density for PF coils, based on superconducting properties and critical surface parameterisation, are also added. This paper highlights these advancements through a case study based on the STEP baseline design.

## 1. Introduction

Fusion has the promise to be a key component of the safe, sustainable, clean and decarbonised energy mix for the future — reducing the reliance on fossil fuels and mitigating the climate crisis. To make this promise a reality, a number of concepts have been explored within the fusion community in the last few decades, one of which is the spherical tokamak concept. With a compact design (lower aspect ratio), high $\beta$ (ratio of plasma pressure to magnetic pressure) and a high bootstrap current (self-generated current by the plasma itself), spherical tokamaks offer efficient plasma confinement, reduced need for external current drives for steady state operation, and a cost effective alternative to conventional tokamaks.

The Spherical Tokamak for Energy Production (STEP) is the UK's public–private programme with the mission to deliver a UK prototype fusion energy plant and a path to the commercial viability of fusion [1,2]. The aim is to produce net energy by 2040, with a target export of 100 MW of electricity (100 MWe) to the grid [3], ensure tritium self-sufficiency, and develop a viable maintenance scheme to support the availability of commercially relevant plants. Achieving this goal requires a structured and adaptive design strategy to navigate the complexities and interdependencies between plasma physics, engineering constraints, and plant integration.

The design process for the STEP prototype follows an iterative, evolution-driven approach. A Concept Maturity Level (CML) structure [4] guides the progression of a design from early-stage concepts to a fully mature and validated system. This is supported by decision-making based on measures of effectiveness—such as net power output, fuel self-sufficiency, safety and environmental factors, maintainability, development flexibility, schedule, and cost [3]—aligning with the programme's performance targets.

To support this, a rapid and integrated workflow is required to manage design challenges, facilitate quick feasibility assessments, and enable the early identification of potential issues. This rapid workflow was previously described in [5], where the PROCESS [6] systems code was used to establish an initial design point using simplified 0-D/1-D models, followed by iterations with the plasma codes JETTO [7] and FIESTA [8] to refine fidelity. Furthermore, Bluemira [9], an open-source multi-fidelity design framework, was used to generate CAD models, integrating these tools into a more cohesive design process.

* Corresponding author.
*E-mail address:* athoy.nilima@ukaea.uk (A. Nilima).

https://doi.org/10.1016/j.fusengdes.2025.115357
Received 4 December 2024; Received in revised form 10 April 2025; Accepted 18 July 2025

**Table 1**
Key Parameters for STEP baseline design.

| | |
|---|---|
| Fusion Power | 1600–1800 MW |
| Net Electric Power | 100–200 MWe |
| Major Radius | 3.6 m |
| Magnetic Field | 3.2 T |
| Elongation | 2.93 |
| Triangularity | 0.5 |
| Inboard Radius | 1.6 m |
| Plasma Current | 20–25 MA |
| Aspect Ratio | 1.8 |
| Tritium Breeding Ratio | 1.17 |

Building upon this foundation, Bluemira has further expanded its capabilities to enhance tokamak design automation and optimisation in recent years. Recent developments include the incorporation of spherical harmonic flux constraints [10], radiation heat load models, first-wall contour designs [11], and critical current models for nested optimisation of the PF coils.

This paper details some of these recent advances in the STEP-Bluemira power plant design framework, highlighting newly integrated critical current constraints and keep-in-zone modules for the nested optimisation of PF coil positions and currents. These functionalities further strengthen Bluemira's role in accelerating the STEP design process.

It is important to note that this paper is not a detailed STEP design study but a demonstration of Bluemira's capabilities to facilitate and accelerate an automated rapid design workflow for the current and ongoing STEP design process, illustrated through a case study based on the STEP baseline design. A more detailed breakdown of the scientific and engineering design concepts for STEP baseline is available in the special issue of Philosophical Transactions A, published by the Royal Society [12].

The paper is structured as follows. A high-level overview of the STEP baseline design is presented in Section 2, followed by the STEP-Bluemira design workflow in Section 3. The critical current models for STEP PF coils and the implementation of these constraints in the optimisation process are discussed in Section 4. Section 5 introduces the keep-in-zone module, which supports the simultaneous refinement of STEP PF coil positions and currents using Bluemira. A demonstration of these capabilities for the STEP baseline design is presented in Section 6, followed by the summary and future outlook in Section 7.

## 2. STEP baseline design: a high-level overview

The STEP baseline concept (CML5 design point) [3] features a spherical tokamak with a double null plasma, a major radius of $3.6\,m$, an aspect ratio of ($A = 1.8$), an inboard radius of $1.6\,m$, high elongation ($\kappa = 2.93$), triangularity ($\delta = 0.5$) and an on-axis magnetic field of $3.2\,T$. The key design parameters are listed in Table 1.

The main driver of this design point was to maximise the inboard build space while minimising the major radius. The compact aspect ratio of this design means that inboard breeding is not feasible. To ensure fuel self-sufficiency with a tritium breeding ratio of 1.17, a helium-cooled liquid lithium breeder blanket is proposed for the outboard region [13]. A double-null configuration with a Super-X outer leg divertor was chosen [14] to effectively manage heat loads, as the double-null setup pushes more power to the outboard side, where the Super-X geometry spreads the heat over a larger area, reducing peak thermal load on the divertor components. Electron Cyclotron (EC) and Electron Bernstein Waves (EBW) were selected for heating and current drive to optimise current drive efficiency while minimising spatial requirements. Since EC requires a high toroidal field and EBW a low field, a toroidal field of 3.2 $T$ was chosen to support both. Achieving this field within the limited major radius required the use of high-temperature superconductor (HTS) magnets [15], with REBCO (Rare Earth Barium Copper Oxide)-based HTS being the preferred choice. HTS conductors operating at $\sim 20\,K$ provide greater thermal capacity than low-temperature superconductors, and their ability to remain superconducting over a wider temperature range enables segmented, resistively jointed TF coils, which are essential for STEP's vertical maintenance approach [16].

The baseline design forms a crucial foundation for STEP, yet there are several key aspects and technology challenges that extend beyond it. As the design evolves, specifications are refined through iterative testing, integrating advanced technologies to enhance performance, and addressing emerging engineering challenges [17]. This paper focuses on the STEP baseline scenario, showcasing Bluemira's added capabilities in the early stages of design maturation within the integrated workflow, as elaborated in the following section.

**Table 2**
Bluemira capabilities.

| |
|---|
| Interface to 0/1-D PROCESS systems code |
| Interface to 1.5-D PLASMOD transport and fixed boundary equilibrium solver |
| 2-D fixed and free boundary equilibrium solvers |
| 3-D magnetostatics solvers |
| 3-D geometry and CAD |
| Simplified dynamic tritium fuel cycle model |
| Axis-symmetric CSG (Constructive solid geometry) CAD models for neutronics [18] |

## 3. STEP-Bluemira design workflow

Bluemira is an integrated, inter-disciplinary and open-source design tool that offers multi-fidelity modelling at different stages in typical tokamak design processes. The STEP-Bluemira design framework leverages these capabilities for spherical tokamaks for the STEP programme. Use of Bluemira for STEP provides design optimisation capabilities at different levels of fidelity throughout the design process. Table 2 lists some of the various capabilities of Bluemira, highlighting its range of tools for design and analysis.

A typical STEP-Bluemira design workflow is illustrated in Fig. 1. For a given STEP design point, the workflow relies on the following inputs:

1. the fixed-boundary equilibrium file from the 1.5D transport code JETTO,
2. the initial radial build from the systems code PROCESS, and
3. a set of configuration and design parameter files specified by the user.

Bluemira provides an integrated interface for running PROCESS and importing its output files directly within the tool. PROCESS includes stress models [19] for the structural materials in the inboard build and outputs the radial build parameters that meet these constraints. Therefore, the radial build parameters read from the PROCESS output are taken as inputs for Bluemira. Once the parameters are read, the global parameter frame (a data-class Bluemira uses to hold a collection of design parameters) is updated and fed into the subsequent design phases.

The design process begins with the fixed-to-free-boundary equilibrium solver. The solver produces an initial free-boundary equilibrium that matches the Last Closed Flux Surface (LCFS) of the fixed-boundary equilibrium obtained from the JETTO output file. Initial PF coil positions, as specified in the configuration files, are used to define preliminary 'keep-in' zones for the magnets (see Section 5). These initial coil positions are typically guided by insights from prior design studies but are subsequently optimised within the defined keep-in zones during the design process.

The workflow then advances to the most computationally intensive phase (several minutes in a laptop): the magnetic cage optimisation loop. This stage involves the coupled optimisation of equilibrium and magnet design, including TF coil ripple optimisation, PF coil position-current optimisation under various engineering constraints, and outer

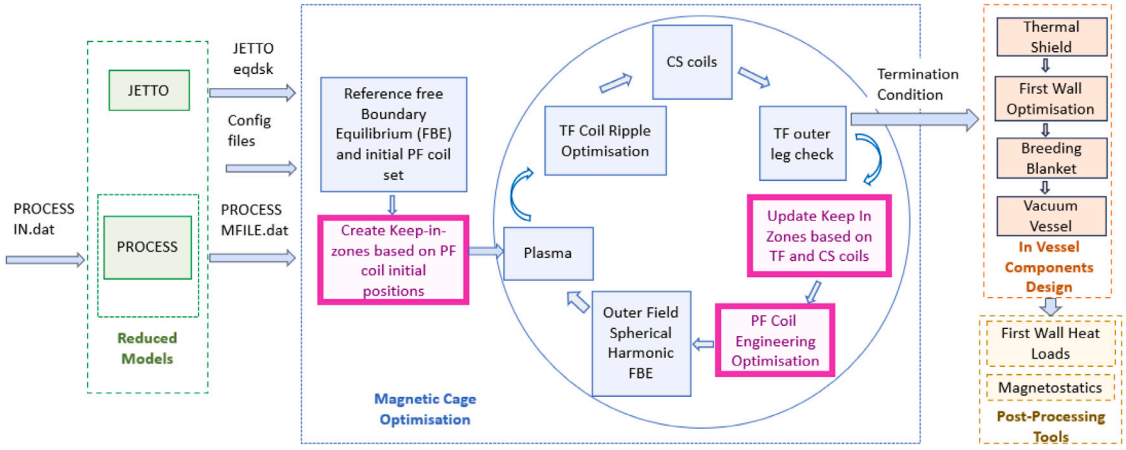


**Fig. 1.** STEP-Bluemira design workflow. Green boxes refer to the external codes that provide design inputs for Bluemira. Blue and pink boxes are the stages of the magnetic cage optimisation loop, with arrows indicating their sequence, and pink highlighting steps relevant to this work. Orange boxes represent the design phases of in-vessel components. Available post-processing tools are colour-coded in yellow. Each step produces output including CAD.

field optimisation, which adjusts PF coil currents to improve the shape of the divertor legs using spherical harmonic constraints [10,20].

The loop continues until a termination condition is met. At present, it compares the positions of the TF coil outboard leg between two consecutive iterations. If the difference falls below a user-defined threshold, the optimisation is considered to be converged, and the loop terminates. Once the magnetic cage design is finalised, the workflow proceeds to designing the thermal shield, first wall (including the divertor), blanket, and vacuum vessel.

The steps relevant to this paper are highlighted in pink in Fig. 1 and elaborated in Sections 4 and 5. Each step generates outputs, including CAD models, that can be integrated into other software for more detailed studies.

## 4. Implementation of critical current constraints in STEP-Bluemira

STEP will employ high-temperature superconducting magnets in its PF coils, with REBCO (Rare Earth Barium Copper Oxide) tapes being the preferred choice. The current in a superconductor is limited by a critical current, i.e. the maximum current a superconducting material can carry while maintaining its superconducting state. It varies from one superconducting material to the other, and depends on the magnetic field conditions and temperature. In real-world applications, the engineering critical current density is of primary interest, as it incorporates not only the intrinsic material properties but also practical engineering factors like tape architecture, cooling efficiency, and safety margin.

### 4.1. Critical current models for a single REBCO Tape

#### 4.1.1. Uglietti scaling law

The field-temperature dependence of the critical current densities of REBCO tapes can be described by the empirical scaling law introduced by Uglietti et al. [21]:

$$J_c(B,T) = A\frac{B_0(T)^{\beta}}{B}\left(\frac{B}{B_0(T)}\right)^{p}\left(1-\frac{B}{B_0(T)}\right)^{q} \tag{1}$$

where $B_0(T) = B_0\left(1-\frac{T}{T_0}\right)^{\alpha}$.

This scaling law includes six fitting parameters ($\alpha$, $\beta$, $p$, $q$, $B_0$, $T_0$) and a scaling parameter $A$. The parameters must be fitted to the specific characterisation data of the REBCO tape in question.

Different sets of parameters fitted to published data by manufacturers are available in literature. For demonstration purposes, two sets of parameters have been included in STEP-Bluemira framework as default:

1. a low $I_c$ parameterisation by Wolf et al. [22], and
2. a high $I_c$ parameterisation by Zhai et al. [23].

Note that the original Uglietti scaling was formulated for the critical current rather than the engineering critical current density, and in this study the necessary adjustment is incorporated into $A$. The parameter A is transformed into a function A(T) [6] based on a Newton polynomial fit considering $A(4.2\ \mathrm{K}) = 2.2\times10^8$, $A(20\ \mathrm{K}) = 2.3\times10^8$ and $A(65\ \mathrm{K}) = 3.5\times10^8$ to fit the data from Hazelton et al. [24].

#### 4.1.2. Durham scaling law

The Uglietti scaling law (1) has been widely adopted for Cross-Conductor (CroCo) and Conductor on Round Core (CORC) cables [22,23]. However, it does not explicitly account for strain dependence in critical current, which can be an important factor in REBCO cable performance. The Durham scaling law was developed as a more comprehensive approach, incorporating strain as a variable using a formulation derived from Ginzburg–Landau theory [25] and experimental parameterisation [26–28]. This makes it applicable to a broader range of REBCO cable designs by considering strain effects, which depend on cable architecture, manufacturing processes, and electromagnetic loads. The model was developed using extensive HTS tape characterisation data from Durham University [27] and is fully compatible with the existing cable-in-conduit superconducting model in system code PROCESS.

The Durham scaling law models the engineering critical current density of superconductors as a function of magnetic field $B$, temperature $T$, and axial strain $\varepsilon$ [27]:

$$J_{c,\mathrm{ENG}}(B,T,\varepsilon_I) = A^*(\varepsilon)\left[T_c^*(\varepsilon_I)(1-t^2)\right]^2 \cdot \left[B_{c2}^*(T,\varepsilon_I)\right]^{n-3}\cdot b^{p-1}(1-b)^q \tag{2}$$

where $t = \frac{T}{T_c}$ and $b = \frac{B}{B_{c2}}$.

Here, $\varepsilon_I$ is the intrinsic strain, $T_c$ is the critical temperature and $B_{c2}$ is the upper critical field. The law includes three flux pinning field scaling parameters ($p$, $q$, $n$), and a strain-dependent parameter $A^*(\varepsilon)$.

Parameters fitted to measurements by Branch et al. [27], Braccini et al. [26], and Chislett-McDonald [28] are included in STEP-Bluemira as defaults. The strain dependences of $T_c$ and $B_{c2}$ are taken from [28]. It is important to note that these default parameters should be used only within their interpolation ranges, i.e. $0\ \mathrm{T} < B < 14\ \mathrm{T}$ and $4.2\ \mathrm{K} < T < 60\ \mathrm{K}$.

Note that these default parameters are for reference only. For STEP, the user must fit the parameters to measurement data that reflect the superconducting properties of REBCO in STEP PF coils under conditions

**Table 3**
Typical PF coils in STEP.

| Coil (upper) | Placements | Functions |
|---|---|---|
| P3 | Inboard of the X–point | Elongation control, plasma triangularity and inner divertor leg shaping |
| P4 | Outboard of the X–point | Simultaneous control of the inboard and outboard divertors |
| P5 | Between the outer divertor and TF coil | Divertor outer leg shaping |
| P6 | Vertically between the outer divertor and the core | Divertor outer leg shaping |
| P7 | Radially outboard | Core plasma shaping |
| S1 | Near the X-divertor null | Divertor inner leg shaping |
| S2 | Above the central solenoid | Divertor inner leg shaping |

as close as reasonably possible to those within STEP. An update on recent progress in understanding REBCO coated conductors in the fusion environment relevant to STEP can be found in [29].

### 4.2. Implementation in Bluemira

To guarantee that the optimised coil currents stay within their operating limits (i.e. the coils stay in superconducting states), it is crucial to include the critical current as a constraint in PF coil current optimisation. Despite HTS comprising only a small fraction of the coil cross-section, its properties play a crucial role in the operational stability of the PF coil, as its superconducting characteristics fundamentally determine the coil's current-carrying capacity.

The engineering critical current densities given by the equations (1) or (2), are used to derive the critical current density limits for a single REBCO tape based on its properties, operating conditions (magnetic field and temperature), and a safety margin (to ensure safe operation and to account for various uncertainties). The framework requires the user to specify these coil properties, select a scaling law (Uglietti or Durham law) with fitted parameters, and the desired safety margin in the configuration files. If no specific model or parameters are provided, the Uglietti scaling law is used by default.

The critical current of a PF coil depends on its design, dimensions, and the combined critical currents of its constituent tapes. Coil dimensions are typically determined by the winding pack design to ensure that the critical current limits are met. At this stage, we are in the early phase of concept generation, where rapid evaluation of multiple design concepts is essential. Consequently, detailed optimisation of the winding pack for each iteration is impractical and has not yet been integrated into the workflow described in Section 3. Instead, we assume conservative cross-sections with safety margins, following [8], and assume uniform current distribution throughout the winding pack.

The critical current density limits are imposed as inequality constraints during PF coil engineering optimisation. In each iteration of the optimisation routine, the critical current density of a single REBCO tape is calculated based on the magnetic field and temperature conditions at the centre of the coil. The current density of the PF coil is then evaluated by comparing the ratio of the total coil current to the effective winding pack area against the critical current density of the individual REBCO tape. If the ratio exceeds the critical current density, within the defined safety margin, the optimisation routine adjusts the design parameters to ensure that the coil operates within the critical current density constraints.

Although the dependence of critical current on field orientation with respect to the tapes is not explicitly considered in the scaling laws used above, we acknowledge that anisotropic effects can influence the performance, and this may be incorporated in future refinements of the code.

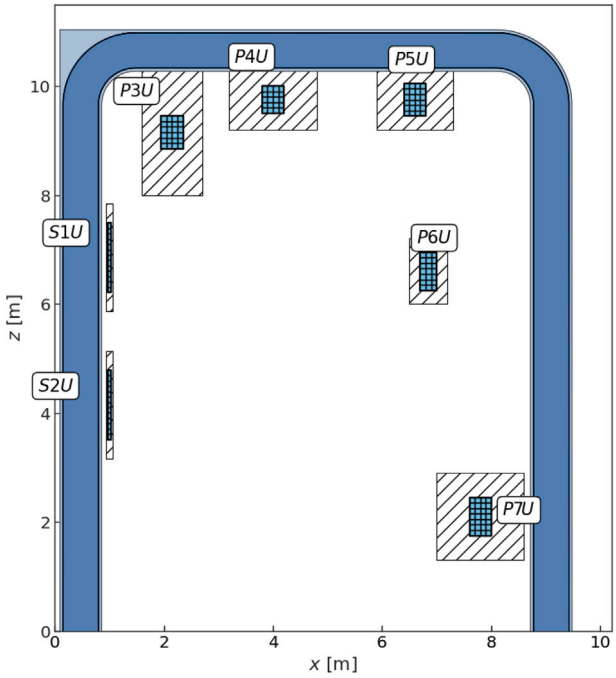


**Fig. 2.** Typical PF coil locations and typical permitted zones (grey) in the upper poloidal plane for the STEP baseline design (unoptimised representation).

## 5. Keep-in-zone module for PF coil position optimisation

STEP will feature seven pairs of PF coils, symmetrically arranged across the $x$-axis at the midplane of the tokamak. A key design choice for STEP is placing all PF coils within the TF cage (but outside the vacuum vessel) [15]. Their proximity to the plasma chamber provides added flexibility, allowing accommodation of a wide range of plasma configurations and advanced divertor geometries, while maintaining relatively low coil currents [8,30]. This is particularly important for advanced exhaust solutions, like the Super-X divertor, which requires additional PF coils to control the extended outer leg and achieve effective poloidal flux expansion for heat load management. Such compact design does impact both inboard shielding and outboard breeding space, but careful consideration was given to strike a balance [3]. Regarding maintenance, STEP will adopt a modular inter-coil structure [15], where each module can be demounted and removed vertically, thanks to the remountable TF coil joints. This modular approach will simplify PF coil maintenance, despite their placement within the magnetic cage.

The initial spatial layout of the coils considers compatibility with TF coils, remote maintenance access, diagnostic port locations, and other in-vessel components. A typical PF coil arrangement in the upper half of the poloidal plane is shown in Fig. 2, based on preliminary radial build assumptions as in [8], with their key functions summarised in Table 3. The P3 coils, situated inboard of the main X-point, manage plasma elongation, maintain high triangularity, and define the inner divertor leg, with their positioning influenced by shielding and divertor configurations. P4 coils balance the inboard and outboard divertors, with their axial placement constrained by the TF coils' height. The P5 and P6 coils jointly shape the outer divertor leg. P5 coils are positioned farther from the plasma to reduce shielding requirements. P6 coils, while closer to the plasma, have strict spatial constraints; being too close to the core plasma can make the last closed flux surface (LCFS) concave, which is undesirable, whereas being too far radially can limit the achievable flux expansion, potentially compromising exhaust performance. The P7 coils generate the vertical field to control plasma radial position, with their placement influenced by the toroidal field coils' radial extent. Additionally, two pairs of quasi-solenoid coils tailor

the inner divertor legs' shape, though their limited space necessitates high current densities and presents engineering challenges.

Optimising the positions of these PF coils, adhering to these spatial constraints, is critical to achieving their intended functions, including the desired plasma shape, divertor control, and overall plasma stability. Bluemira has the capability of nested current-position optimisations, given user-defined "keep-in-zones", as discussed in the following sections.

### 5.1. Nested current-position optimisation for PF coils

The nested current-position optimisation method, originally developed for pulsed tokamaks in Bluemira [9], has been adapted in this work for non-pulsed spherical tokamaks. This method optimises coil positions and currents separately, with the current optimisation nested within the position optimisation. The PF coil positions are optimised within user-defined two-dimensional keep-in-zones, the optimisation objective being that of the current sub-optimisation problem. The objective function of the current optimisation is user-defined and tailored to the specific goals of the design study. For instance, the objective could be to minimise coil currents or to reduce the error in achieving a set of magnetic field targets, with regularisation on currents (a penalty term) to avoid excessively large values. The current sub-optimisation problem typically involves one or more constraints.

The nested current-position optimisation assumes the plasma is *fixed* and that the plasma's effect on various constraints remains largely unchanged during the subsequent equilibrium convergence. This assumption holds as the input equilibrium is always a previously converged solution of the Grad-Shafranov (GS) equation [31]. For instance, the first iteration uses the initial free-boundary equilibrium from the fixed-to-free boundary solver, while subsequent iterations use the converged equilibrium from the prior outer field optimisation phase. This approach accelerates the overall optimisation process.

After optimising positions and currents for a fixed plasma, a Picard iteration scheme re-solves the GS equation and re-optimises currents. Together, the nested optimisation and the Picard iteration scheme constitute the PF coil engineering optimisation phase within the workflow in Fig. 1.

### 5.2. Keep-in-zone module

To apply the nested current-position optimisation for STEP, a dedicated keep-in-zone module has been developed. The module defines rectangular zones in the xz-plane and lets users select which PF coils to optimise. The dimensions of the keep-in-zones are customisable: users can set initial values to guide the optimisation process.

Throughout the magnetic cage optimisation loop, the keep-in-zone module automatically adjusts zone dimensions when clashes are detected with components such as the central solenoid (CS) or the TF coils. For instance, the initial keep-in-zones (Fig. 2) are created with respect to the initial coilset positions prior to the start of magnetic cage optimisation (see Fig. 1). However, as the TF and CS coils are designed, or if changes occur (e.g., shifts in the outer leg position of the TF coils during ripple optimisation), these zones must be dynamically resized. This iterative adjustment avoids clashes with components while ensuring optimal magnetic configuration and maintaining tokamak performance.

The keep-in zones are incorporated into the position optimisation phase using the position-mapping tool of Bluemira [9]. The position mapper uses a set of geometry interpolators to convert the (x,z) coordinates to normalised parametric-space values and vice-versa. In each iteration of the outer loop of the nested optimisation, the optimiser updates the coil positions based on the objective function, using the position mapper to convert the updated parametric-space values back to (x, z) coordinates. This process continues until the optimiser converges, minimising the figure of merit. Bluemira supports a number of optimisation algorithms, based on the Non-Linear Optimisation (NLOpt) [32] library. The users can specify their choice of the algorithm and optimisation conditions (e.g. the maximum number of iterations, tolerances etc.) in the configuration files.

## 6. Case study

This section demonstrates how the keep-in-zones and critical currents are applied in the PF coil engineering optimisation within the STEP-Bluemira design workflow for the STEP baseline design.

The output file from a previous PROCESS run and the fixed-boundary equilibrium file from JETTO corresponding to the Baseline configuration are used as inputs. Fig. 3(a) and Fig. 3(b) illustrate the radial build from PROCESS and the fixed-boundary equilibrium from JETTO respectively. The design parameters, build configuration, and initial estimates for coilset currents and positions are also provided as inputs. We take the initial coilset definitions from previous design points, which are shown in Fig. 3(c).

Adhering to the design workflow outlined in Section 3, the first phase of the magnetic cage loop involves solving an unconstrained Tikhonov Current Gradient problem using the fixed-to-free boundary equilibrium solver. The objective is to optimise the current gradient vector, minimising the error in the L2-norm of a set of isoflux points. This solution provides a sensible initial guess for the starting equilibria, referred to as the reference free boundary equilibrium, which helps accelerate the subsequent optimisation process. The reference free boundary equilibrium is then used to inform the subsequent stages of the magnetic cage loop, which include the design and optimisation of both the equilibrium and the magnets.

The optimisation process begins by defining the keep-in-zones for the coils whose positions are to be optimised. In this particular demonstration, coils 3, 4, and 6 were selected for position optimisation, with their locations adjusted to remain within these predefined zones. Due to the symmetric design of the coilset, the positions of the corresponding coils along the negative $z$ axis were automatically adjusted to mirror those on the positive $z$ axis. COBYLA (Constrained Optimisation BY Linear Approximations) algorithm [33], a gradient-free method, was chosen for position optimisation due to its stability and minimal need for parameter tuning. This position optimisation is part of the Engineering optimisation stage (see bottom right pink box in Fig. 1), which employs the nested optimisation approach (see Section 5.1). In this approach, position optimisation serves as the upper-level optimisation, while current optimisation is treated as the nested sub-optimisation for each evaluation of the coil positions.

For each evaluation of the positions of the selected optimisation coils (coils 3, 4, 6, and their symmetric counterparts), the currents of *all* PF coils were optimised. At each step, the total magnetic field at the PF coil centre coordinates was determined, and the critical current densities were calculated for that field at a default assumed temperature of approximately 5.5 K (chosen to provide a conservative margin for critical currents). These critical current densities were then applied as constraints to ensure that the optimised coil currents remained within operational limits. A Sequential Least Squares Quadratic Programming (SLSQP) algorithm [34] was chosen for current optimisation. SLSQP uses gradient information to achieve faster convergence and is particularly effective for problems with constraints.

The current sub-optimisation problem (and hence the nested optimisation) was assessed using a figure of merit that combined the L2 norm of the error in the magnetic field targets with Tikhonov regularisation applied to the coil currents. A set of isoflux points on the LCFS and the LCFS null points were chosen as the magnetic targets. The Tikhonov regularisation stabilises the solution by penalising large coil currents. This was particularly useful in supporting the design of an extended divertor leg shape (see the right plot in Fig. 4(a)), where the focus

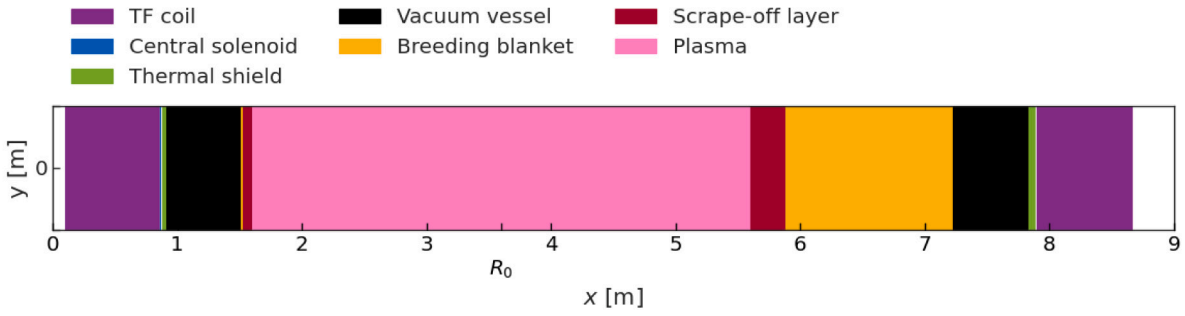


(a) PROCESS Radial Build for STEP Baseline Design

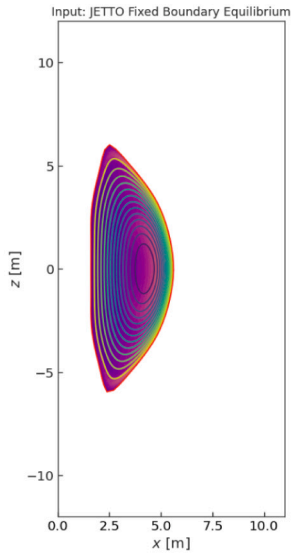


(b) JETTO Fixed boundary equilibrium

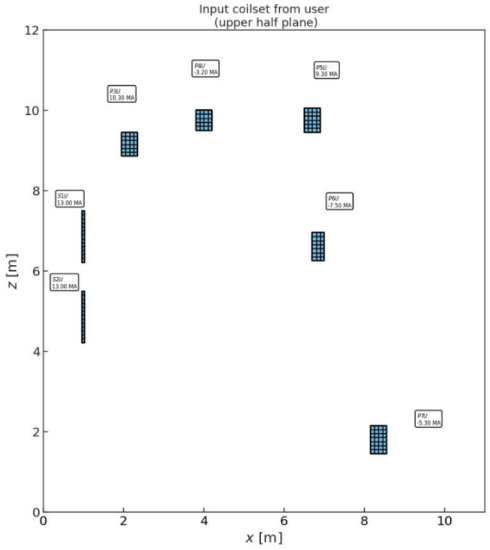


(c) Input Coilset

**Fig. 3.** Inputs to the workflow.

was placed on achieving the desired magnetic field configuration rather than minimising the coil currents.

The final optimised equilibrium and updated coilset positions at the end of the magnetic cage loop are shown in the right plot of Fig. 4(a). Fig. 4(b) illustrates the relative differences in the poloidal magnetic flux between the reference and optimised equilibria, providing an indication of the optimisation's impact on the magnetic configuration.

A zoomed comparison of the coilset before and after optimisation can be seen in Fig. 5, where the colours red and blue correspond to the reference and optimised coilset. As seen in the zoomed comparison, the initial keep-in-zones (red shaded boxes) for the coils P3 and P4 were found to overlap with the TF coils, prompting a dynamic resizing of these zones during the optimisation process, as indicated by the black-shaded resized zones. While the initial keep-in-zone dimensions were set based on approximate spatial considerations of other components, the optimisation process allowed for subtle adjustments where necessary, ensuring the final design is both feasible and optimally configured. The figure also shows that the optimisation process pushed the PF coils right up to the spatial limits defined by their keep-in-zones, implying that the available spatial envelope is being fully utilised. This indicates that the design is tightly constrained by the keep-in-zone boundaries.

In this study, we assumed that the sizes of the PF coils were fixed, and the optimisation focused solely on adjusting the currents and positions of the selected PF coils. As a result, despite the currents in the PF coils changing (e.g., PF3's current decreases from 10.72 MA to 5.75 MA), its cross-sectional area remained unchanged, since coil size was not optimised in this case. Future work will include optimisation of PF coil sizes as well.

The implemented features, including the keep-in-zone for nested optimisation and the critical current constraint in the PF coil engineering optimisation phase, play a key role in the overall magnetic cage optimisation loop. These features ensure that the desired magnetic field configuration is achieved while maintaining engineering feasibility. This also supports further design goals, such as the design of an extended divertor leg shape for STEP. A detailed study on divertor design with STEP-Bluemira is ongoing and will be addressed in future publications.

## 7. Summary and future outlook

The paper outlined some of the newly added functionalities in the STEP-Bluemira power plant design framework, focusing on critical current constraints and a keep-in-zone module to facilitate nested optimisation of PF coil currents and positions.

Two critical current models for REBCO have been added: the widely used Uglietti law [21] and the more recent Durham law [26–28], which accounts for a range of cable designs and strain dependence. Both models provide users the option to input parameters based on the specific characterisation data of the REBCO tape being used. This is particularly important because the characterisation data for REBCO coated conductors for STEP are still unavailable, and the parameters fitted to these data should be used when applying them.

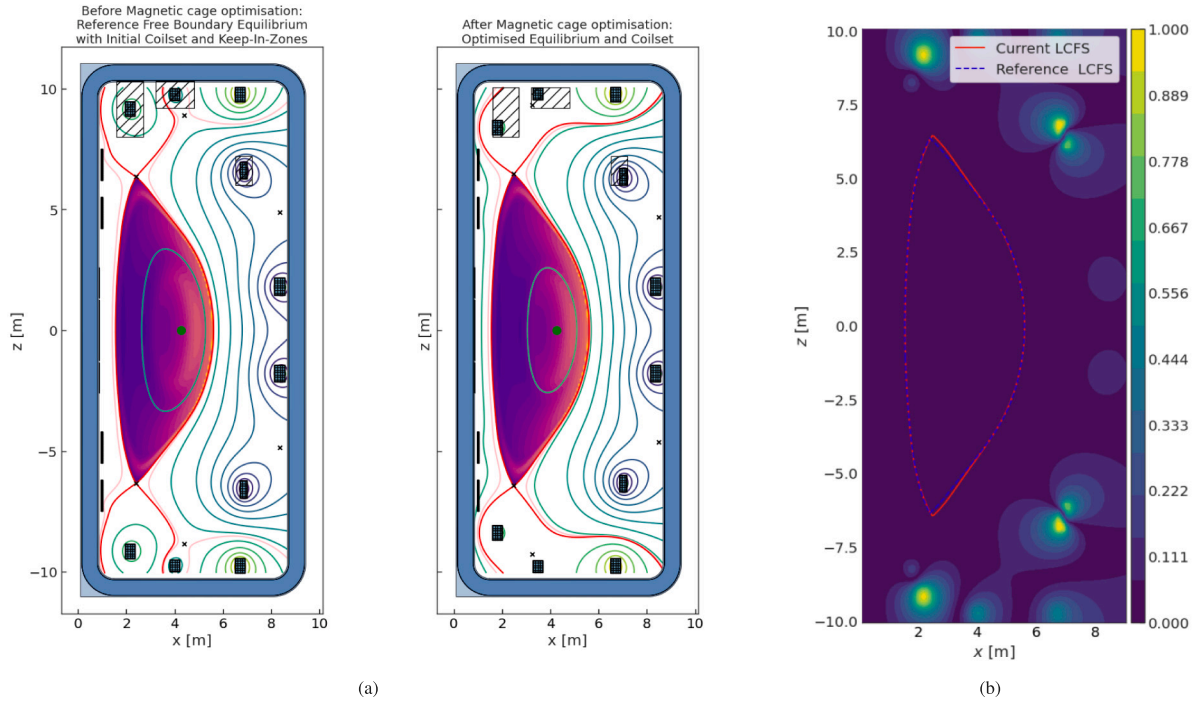


**Fig. 4.** (a) Equilibria and coilset: before (left) and after (right) the magnetic cage optimisation. (b) Relative difference in poloidal magnetic flux between reference and optimised equilibria.

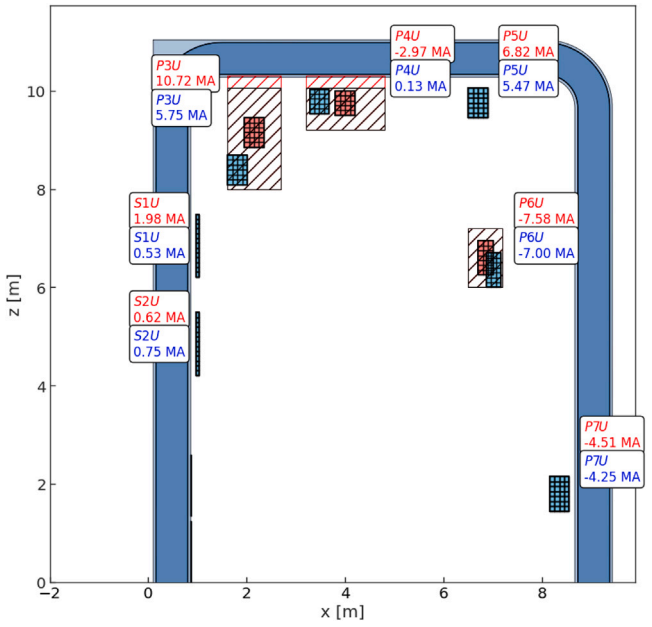


**Fig. 5.** A zoomed-in view of the reference (red) and optimised (blue) coils in the upper poloidal plane after magnetic cage optimisation. The red shaded boxes indicate the reference keep-in zones provided by the user, while the black shaded boxes show the updated zones after correcting for overlaps with the TF coil.

A key challenge in PF coil designs is optimising the positions of PF coils. A customisable keep-in-zone module has been integrated into the STEP-Bluemira framework that allows users to define regions in the XZ plane for coil position optimisation, enabling dynamic resizing in relation to other components throughout the magnetic cage optimisation loop. It also permits the optimisation of a subset of coils instead of the entire set.

The case study demonstrated in the paper gives a simple example of the magnetic cage optimisation with Bluemira, focusing on the keep-in-zones and critical current constraints applied in the PF coil engineering optimisation phase. Detail descriptions of individual stages within and after the loop are subject to future publications.

Moving forward, the framework will be expanded to account for PF coil winding pack design and a refined critical current calculation based on it. Currently, heat load calculations on PF coils are not included in our workflow, but we plan to address this in future studies. Detailed neutronic simulations are planned to evaluate the neutronic heat loads on the coils under various operational scenarios. Further refinement of the keep-in-zone regions will focus on providing adequate shielding from neutron flux, preserving the structural integrity and superconducting performance of the PF coils.

## CRediT authorship contribution statement

**Athoy Nilima:** Software, Methodology, Investigation, Formal analysis, Data curation, Conceptualization, Writing – original draft, Visualization, Validation. **Matthew Bluteau:** Software. **James Cook:** Software, Conceptualization. **Oliver Funk:** Software, Visualization. **Georgina Graham:** Writing – review & editing, Visualization, Software. **Jonathan Matthews:** Software. **Stuart I. Muldrew:** Writing – review & editing, Supervision, Resources, Conceptualization. **Alexander J. Pearce:** Writing – review & editing, Supervision, Conceptualization. **Dario Vaccaro:** Writing – review & editing, Software.

## Declaration of competing interest

The authors declare that they have no known competing financial interests or personal relationships that could have appeared to influence the work reported in this paper.

## Acknowledgements

This work has been funded by STEP, a major technology and infrastructure programme led by UK Industrial Fusion Solutions Ltd (UKIFS), which aims to deliver the UK's prototype fusion powerplant and a path to the commercial viability of fusion.

The authors are grateful to Alexander Petrov (Integrated Magnets Team Lead, UKAEA) for the polynomial fit to A(T) in Eq. (1).

## Data availability

The data that has been used is confidential.

## References

[1] UK Atomic Energy Authority, Department for Business, Energy & Industrial Strategy, The Rt Hon Andrea Leadsom, UK to take a big 'STEP' to fusion electricity, 2019, Press release.

[2] A. Baker, The spherical tokamak for energy production (STEP) in context: UK public sector approach to fusion energy, Philos. Trans. A 382 (2280) (2024) 20230401.

[3] C. Waldon, S.I. Muldrew, J. Keep, R. Verhoeven, T. Thompson, M. Kisbey-Ascott, Concept design overview: a question of choices and compromise, Philos. Trans. R. Soc. A: Math. Phys. Eng. Sci. 382 (2024) http://dx.doi.org/10.1098/rsta.2023.0414.

[4] R. Wessen, C.S. Borden, J.K. Ziemer, R.C. Moeller, J. Ervin, J. Lang, Space mission concept development using concept maturity levels, in: AIAA SPACE 2013 Conference & Exposition, American Institute of Aeronautics and Astronautics, 2013, http://dx.doi.org/10.2514/6.2013-5454.

[5] S.I. Muldrew, C. Harrington, J. Keep, C. Waldon, C. Ashe, R. Chapman, C. Griesel, A.J. Pearce, F. Casson, S.P. Marsden, E. Tholerus, Conceptual design workflow for the STEP prototype powerplant, Fusion Eng. Des. 201 (2024) 114238, http://dx.doi.org/10.1016/j.fusengdes.2024.114238.

[6] J. Morris, S. Muldrew, P. Knight, M. Kovari, A. Pearce, S. Kahn, J. Maddock, T. Nunn, R. Chapman, C. Swanson, H. Lux, J. Foster, K. Ellis, M. Kumar, G. Turkington, J. Lion, S. Chislett-McDonald, A. Brown, J. Edwards, C. Ashe, E. Fable, K. Zarebski, C. Griesel, R. Kemp, S. Gubbins, S. Pickering, J. Matthews, G. Graham, C. Mould, T. Miller, S. Gadgil, D. Short, J. Cook, P. Lloyd, Process, 2024, URL https://github.com/ukaea/PROCESS.

[7] G. Cenacchi, A. Taroni, JETTO: A Free Boundary Plasma Transport Code, Tech. Rep. ENEA-RT-TIB–88-5, ENEA, Bologna (Italy). Centro Ricerche Energia, Italy, 1988, 84 pages.

[8] A. Hudoba, G. Cunningham, S. Bakes, Magnetic equilibrium optimisation and divertor integration in spherical tokamak reactors, Fusion Eng. Des. 191 (2023) 113704, http://dx.doi.org/10.1016/j.fusengdes.2023.113704.

[9] M. Coleman, J.E. Cook, F. Franza, I.A. Maione, S. McIntosh, J. Morris, D. Short, A.I. Blair, M. Bluteau, H. Brooks, I. Chiang, S. Desai, M. Foord, O. Funk, G.A. Graham, J. Hagues, L. Humphrey, M. Johnson, S. Kahn, C. MacMackin, S. Mason, H. Saunders, D. Vaccaro, O. Wong, Bluemira, URL https://github.com/Fusion-Power-Plant-Framework/bluemira.

[10] G. Graham, O. Bardsley, S. Khan, A. Pearce, M. Johnson, Conceptual design of spherical tokamaks using spherical harmonic flux constraints in Bluemira, in: IEEE Symposium on Fusion Engineering, SOFE, IEEE, Oxford, 2023, Poster.

[11] D. Vaccaro, J. Cook, S. Kahn, T. Barrett, M. Bluteau, M. Coleman, F. Federici, S. Henderson, D. Horsley, A. Hudoba, M. Kovari, R. Osawa, A. Pearce, M. Richiusa, D. Short, M. Subramani, K. Verhaegh, Z. Vizvary, F. Bagnato, D. Galassi, S. Minucci, Models implemented in the methodological approach to design the initial STEP first wall contour, Fusion Eng. Des. 204 (2024) 114479, http://dx.doi.org/10.1016/j.fusengdes.2024.114479.

[12] Theme issue: Delivering fusion energy – The spherical tokamak for energy production (STEP), Philos. Trans. R. Soc. A: Math. Phys. Eng. Sci. 382 (2280) (2024) URL https://royalsocietypublishing.org/toc/rsta/2024/382/2280, Compiled and edited by Prof. Sir Ian Chapman, Prof. Sir Steven Cowley, and Prof. Howard Wilson.

[13] M. Lord, I. Bennett, C. Harrington, A. Cooper, D. Lee-Lane, A. Cureton, C. Olde, M. Thompson, D. Jayasundara, T. Meatyard, Fusing together an outline design for sustained fuelling and tritium self-sufficiency, Phil. Trans. R. Soc. A 382 (2024) http://dx.doi.org/10.1098/rsta.2023.0410.

[14] J. Cane, A. Barth, J. Farrington, E. Flynn, S. Kirk, J. Lilburne, Z. Vizvary, Managing the heat: In-vessel components, Phil. Trans. R. Soc. A 382 (2024) 20230408, http://dx.doi.org/10.1098/rsta.2023.0408.

[15] E. Nasr, S. Wimbush, P. Noonan, P. Harris, R. Gowland, A. Petrov, The magnetic cage, Philos. Trans. A 382 (2280) (2024) 20230407.

[16] A. van Arkel, C. Lamb, H. Robinson, Y. Dieudonné, Unlocking maintenance—architecting STEP for maintenance and realizing remountable magnet joints, Phil. Trans. R. Soc. A 382 (2213) (2024) 20230415, http://dx.doi.org/10.1098/rsta.2023.0415.

[17] D. Kempton, C. Waldon, Maturing the design: challenges in maturing a first of a kind fusion power plant, Phil. Trans. R. Soc. A 382 (20230412) (2024) http://dx.doi.org/10.1098/rsta.2023.0412.

[18] O. Wong, J. Cook, J. Hagues, M. Coleman, Application of high throughput neutronics simulation in fusion power plant design framework Bluemira, in: 15th ITER Neutronics Meeting and Fusion Neutronics Workshop, 2024, 10/04/2024.

[19] M. Kovari, F. Fox, C. Harrington, R. Kembleton, P. Knight, H. Lux, J. Morris, "Process": A systems code for fusion power plants – part 2: Engineering, Fusion Eng. Des. 104 (2016) 9–20, http://dx.doi.org/10.1016/j.fusengdes.2016.01.007.

[20] O.P. Bardsley, J.L. Baker, C. Vincent, Decoupled magnetic control of spherical tokamak divertors via vacuum harmonic constraints, Plasma Phys. Control. Fusion 66 (5) (2024) 055006, http://dx.doi.org/10.1088/1361-6587/ad319d.

[21] D. Uglietti, N. Bykovsky, K. Sedlak, B. Stepanov, R. Wesche, P. Bruzzone, Test of 60 ka coated conductor cable prototypes for fusion magnets, Supercond. Sci. Technol. 28 (12) (2015) 124005, http://dx.doi.org/10.1088/0953-2048/28/12/124005.

[22] M.J. Wolf, N. Bagrets, W.H. Fietz, C. Lange, K.-P. Weiss, Critical current densities of 482 $A/mm^2$ in HTS CrossConductors at 4.2 k and 12 t, IEEE Trans. Appl. Supercond. 28 (4) (2018) 1–4, http://dx.doi.org/10.1109/TASC.2018.2815767.

[23] Y. Zhai, D. van der Laan, P. Connolly, C. Kessel, Conceptual design of HTS magnets for fusion nuclear science facility, Fusion Eng. Des. 168 (2021) 112611, http://dx.doi.org/10.1016/j.fusengdes.2021.112611.

[24] D. Hazelton, 2G HTS wire development at SuperPower, 2017, URL https://indico.cern.ch/event/588810/contributions/2473740/, Presented at CERN.

[25] W.H. Kleiner, L.M. Roth, S.H. Autler, Bulk solution of Ginzburg-Landau equations for type II superconductors: Upper Critical Field Region, Phys. Rev. 133 (1964) A1226–A1227, http://dx.doi.org/10.1103/PhysRev.133.A1226.

[26] V. Braccini, A. Xu, J. Jaroszynski, Y. Xin, D.C. Larbalestier, Y. Chen, G. Carota, J. Dackow, I. Kesgin, Y. Yao, A. Guevara, T. Shi, V. Selvamanickam, Properties of recent IBAD–MOCVD coated conductors relevant to their high field, low temperature magnet use, Supercond. Sci. Technol. 24 (3) (2010) 035001, http://dx.doi.org/10.1088/0953-2048/24/3/035001.

[27] P. Branch, K. Osamura, D. Hampshire, Weak emergence in the angular dependence of the critical current density of the high temperature superconductor coated conductor REBCO, Supercond. Sci. Technol. 33 (10) (2020) 104006, http://dx.doi.org/10.1088/1361-6668/abaebe.

[28] S. Chislett-McDonald, Designing a Fusion Power Plant with Superconducting Training Magnets (Ph.D. thesis), Durham University, 2022.

[29] W. Iliffe, S. Chislett-McDonald, F. Harden, K. Adams, J. Tufnail, C. Grovenor, S. Speller, A. Reilly, S.C. Wimbush, E. Nasr, Progress in the STEP programme toward understanding REBCO coated conductors in the fusion environment, IEEE Trans. Appl. Supercond. 35 (5) (2025) 1–5, http://dx.doi.org/10.1109/TASC.2024.3523248.

[30] A. Hudoba, S. Newton, G. Voss, G. Cunningham, S. Henderson, Divertor optimisation and power handling in spherical tokamak reactors, Nucl. Mater. Energy 35 (2023) 101410, http://dx.doi.org/10.1016/j.nme.2023.101410.

[31] H. Grad, H. Rubin, Hydromagnetic equilibria and force-free fields, J. Nucl. Energy 7 (1958) 284–285.

[32] S.G. Johnson, The nlopt nonlinear-optimization package, 2008, URL https://github.com/stevengj/nlopt.

[33] M.J.D. Powell, A direct search optimization method that models the objective and constraint functions by linear interpolation, in: Advances in Optimization and Numerical Analysis, Springer Netherlands, Dordrecht, 1994, pp. 51–67, http://dx.doi.org/10.1007/978-94-015-8330-5_4.

[34] D. Kraft, A Software Package for Sequential Quadratic Programming, Tech. Rep. DFVLR-FB 88-28, Deutsche Forschungs- und Versuchsanstalt für Luft- und Raumfahrt, 1988.